Design and Analysis of a Plug-In Robust Compensator: An Application to Indirect-Field-Oriented-Control Induction Machine Drives

Wai-Chuen Gan, *Member, IEEE*, and Li Qiu, *Senior Member, IEEE*

***Abstract*—It is well known that the system performance for an indirect-field-oriented-control induction motor drive degrades under the variation of rotor resistance and in the presence of external load torque. In this paper, a plug-in robust compensator for speed and position control enhancement of an indirect-field-oriented-control induction machine drive is developed. In the case where a controller for the induction machine already exists or is in operation with satisfactory nominal tracking performance, this plug-in compensator, designed using the $\mathcal{H}_\infty$ loop-shaping techniques, can be plugged into the existing controller without affecting the already satisfactory nominal tracking performance of the existing closed-loop system but with the capability to improve the system performance under plant parameter variations and in the presence of external disturbances. Simulation and experimental results are given to validate the proposed plug-in robust compensator.**

***Index Terms*—$\mathcal{H}_\infty$ loop-shaping design, indirect-field-oriented-control induction machine drive, plug-in robust compensator, rotor resistance change.**

I. Introduction

A ROBUST MOTOR control system should exhibit good speed and position tracking and disturbance rejection even under plant parameter variations. Although indirect-field-oriented control (IFOC) can transform a nonlinear induction motor into a linear system [1], it is well known that under IFOC, the output response is sensitive to the plant parameter variations such as rotor resistance change [2]. Different approaches have been applied to tackle the plant parameter variation problem.

In [3], $\mathcal{H}_\infty$ mixed-sensitivity optimization is applied to solve the plant parameter variation problem; however, weighting function selection is not an easy task and the order of the final controller, which is designed by $\mathcal{H}_\infty$ mixed-sensitivity optimization, is usually high. In [4], a fuzzy logic control approach is employed to enhance the system robustness but the design of proper fuzzy rules is not straightforward and the knowledge from a skillful tuning operator may be needed to generate meaningful fuzzy rules. In [5], an adaptive scheme is developed to estimate the rotor resistance so that the output speed performance can still be guaranteed when the rotor resistance changes during operation. However, the zero external torque assumption required by this adaptive controller may not be valid in real applications and its computational burden may be too demanding for a low-cost digital signal processor (DSP)/microcontroller. Furthermore, the tracking performance and the system robustness cannot be designed separately in [3]–[5]. As in many cases, the nominal/existing controllers for tracking performance are in operation or already designed properly by employing a low-order and simple controller such as proportional–derivative (PD), proportional–integral (PI), proportional–integral–derivative (PID), or lead/lag compensators. However, these controllers may not have sufficient robustness against plant parameter variations or external disturbance such as the rotor resistance change in an IFOC induction motor system; hence, a good way to solve this problem is to design a plug-in compensator which can enhance the system robustness without affecting the nominal tracking performance.

The idea of plug-in compensators is based on the Youla parameterization of all two-degrees-of-freedom (2DOF) stabilizing controllers [15]. The parameterization can be constructed from the existing controller in such a way that one of the free parameters in the 2DOF structure has no effect on the nominal tracking performance but can be used to improve, among other things, the feedback loop robustness against plant uncertainties and external disturbances. The use of certain versions of such plug-in compensators has been reported in [6], [7], [9], and [17] with successful applications in dc motor control, control of a gyroscope system, and vibration suppression control. The design of a plug-in compensator boils down to the design of the free parameter in the Youla parameterization. In our application, we wish to use the plug-in compensator to improve the robustness of the closed-loop system against the rotor resistance change in an IFOC induction motor drive and against the external torque disturbances. Since the rotor resistance enters the linear model of the IFOC system in a highly nonlinear way and there are possibly other parameter uncertainties from unknown sources, it is very hard to obtain the structural and magnitude information of the uncertainties. Therefore, we propose to use the $\mathcal{H}_\infty$ loop-shaping design technique [10], [11], [13] to

Manuscript received August 27, 2001; revised June 10, 2002. Abstract published on the Internet February 4, 2003. This work was supported by the Hong Kong Research Grants Council under Grant HKUST6032/01E.

W.-C. Gan was with the Department of Electrical and Electronic Engineering, The Hong Kong University of Science and Technology, Hong Kong. He is now with ASM Assembly Automation Ltd., Hong Kong.

L. Qiu is with the Department of Electrical and Electronic Engineering, The Hong Kong University of Science and Technology, Hong Kong (e-mail: eeqiu@ee.ust.hk).

Digital Object Identifier 10.1109/TIE.2003.809393

design the plug-in compensator. Theoretically, this technique is optimal in dealing with unstructured uncertainty described by the gap metric or the ν-gap metric. Practically, it is effective in cases when the uncertainty has unknown sources and is hard to measure. Comparing to other $\mathcal{H}_\infty$ controller design methods such as mixed sensitivity optimization, the loop-shaping design turns the difficult task of external weighting function selection into the relatively easy choice of loop-shaping functions and eliminates the time-consuming γ-iteration, which is required in usual $\mathcal{H}_\infty$ optimization, in the computation of the optimal controller.

This paper is organized as follows. Section II gives a brief review on the IFOC of induction motors and the detuning of IFOC driver systems. In Section III, the structure for the plug-in robust compensator is first introduced and then a systematic design procedure is given. Section IV presents the simulation results of the proposed controller. In Section V, experimental results are compared with the simulation results to validate our control methodology. Some concluding remarks are given in Section VI.

II. IFOC of Induction Motors

The modeling and IFOC of induction motors are reviewed in this section. A three-phase squirrel-cage induction motor can be modeled in $d-q$ frame by the following equations [1]:

stator voltage balancing equations

$$v_{ds} = (R_s + L_s p) i_{ds} - \omega_e L_s i_{qs} + L_m p i_{dr} - \omega_e L_m i_{qr} \quad (1)$$

$$v_{qs} = \omega_e L_s i_{ds} + (R_s + L_s p) i_{qs} + \omega_e L_m i_{dr} + L_m p i_{qr} \quad (2)$$

flux linkage equations

$$\begin{aligned} \lambda_{ds} &= L_s i_{ds} + L_m i_{dr} \\ \lambda_{qs} &= L_s i_{qs} + L_m i_{qr} \\ \lambda_{dr} &= L_r i_{dr} + L_m i_{ds} \\ \lambda_{qr} &= L_r i_{qr} + L_m i_{qs} \end{aligned}$$

rotor voltage balancing equations

$$\begin{aligned} 0 &= R_r i_{dr} + p\lambda_{dr} - (\omega_e - \omega_r)\lambda_{qr} \\ 0 &= R_r i_{qr} + p\lambda_{qr} + (\omega_e - \omega_r)\lambda_{dr} \end{aligned}$$

torque equations

$$\begin{aligned} \tau_e &= \frac{3}{2}\frac{P}{2}\frac{L_m}{L_r}(\lambda_{dr} i_{qs} - \lambda_{qr} i_{ds}) \\ \tau_e &= J_m p\omega_{rm} + B_m \omega_{rm} + \tau_l \\ \omega_r &= \frac{P}{2}\omega_{rm}. \end{aligned}$$

Here, the parameters and variables have the following meanings:

v_{ds}, v_{qs}	d–q-axes stator voltages;
i_{ds}, i_{qs}	d–q-axes stator currents;
i_{dr}, i_{qr}	referred d–q-axes rotor currents;
λ_{ds}, λ_{qs}	d–q-axes stator fluxes;
λ_{dr}, λ_{qr}	referred d–q-axes rotor fluxes;
ω_e	abc to d–q frame transformation velocity;
ω_r	rotor electrical velocity;
ω_{rm}	rotor mechanical velocity;
τ_e	electromechanical torque;
τ_l	load torque;
$p = d/dt$	differentiation operator;
R_s	stator resistance;
L_s	stator inductance;
R_r	referred rotor resistance;
L_r	referred rotor inductance;
L_m	mutual inductance;
P	number of poles (even number);
J_m	moment of inertia;
B_m	friction constant.

The stator voltage balancing equations (1) and (2) can be neglected if we use a fast current-regulated voltage-source inverter. The stator currents i_{ds} and i_{qs} then become the new control input variables. IFOC is an effective linearization control algorithm for a highly nonlinear induction motor [1]. With the rotor flux oriented at the d axis, i.e., $\lambda_{qr} = 0$, the above nonlinear equations can be transformed onto the $d-q$ synchronous frame and described by the following equations:

$$L_r i^e_{qr} + L_m i^e_{qs} = 0 \quad (3)$$

$$L_r i^e_{dr} + L_m i^e_{ds} = \lambda^e_{dr} \quad (4)$$

$$R_r i^e_{dr} + p\lambda^e_{dr} = 0 \quad (5)$$

$$R_r i^e_{qr} 0 + (\omega_e - \omega_r)\lambda^e_{dr} = 0 \quad (6)$$

$$\tau_e = \frac{3}{2}\frac{P}{2}\frac{L_m}{L_r}\lambda^e_{dr} i^e_{qs} = J_m p\omega_{rm} + B_m\omega_{rm} + \tau_l \quad (7)$$

$$(\omega_e - \omega_r) = \frac{R_r}{L_r}\frac{L_m i^e_{qs}}{\lambda^e_{dr}} \quad (8)$$

where

i^e_{ds}, i^e_{qs}	d–q synchronous axes stator currents;
i^e_{dr}, i^e_{qr}	d–q synchronous axes rotor currents;
λ^e_{dr}, λ^e_{qr}	d–q synchronous axes rotor fluxes.

Fig. 1(a) shows the general block diagram of an indirect-field-oriented induction machine drive. By using IFOC, a highly nonlinear induction motor can be converted into a linear system. Fig. 1(b) is the block diagram representation of the linearized induction motor. In the diagram, $u = \tau_e$ is the command torque input, y is the system output which can select between ω_{rm} or θ_{rm} for speed and position control, respectively, $d = \tau_l$ is the external disturbance, and τ_l is assumed to be a constant load torque. The rotor flux λ^e_{dr} is assumed to be kept at a constant value.

Note that the calculation of the slip frequency $(\omega_e - \omega_r)$ in (8) depends on the rotor resistance. Owing to saturation and heating, the rotor resistance changes and hence the slip frequency is either over or under estimated. Eventually, the rotor flux λ^e_{dr} and the stator q-axis current i^e_{qs} will be no longer decoupled in (7) and the instantaneous torque control is lost. Furthermore, the electromechanical torque generation is reduced at steady state under the plant parameter variations and hence the machine will work in a low-efficiency region [1], [2]. Finally, the variation of the parameters J_m and B_m is common in real applications. For instance, the bearing friction will change after the motor has run for a period of time.

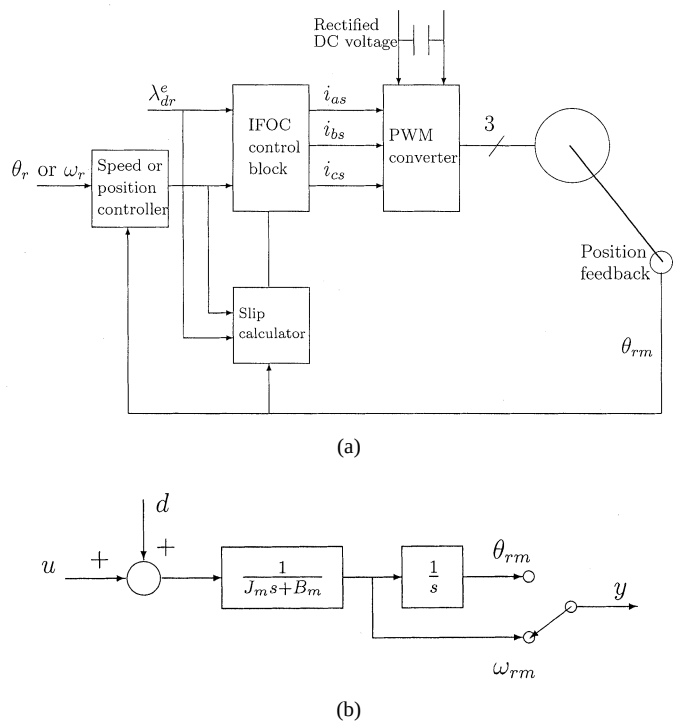

Fig. 1. (a) Block diagram of an IFOC induction machine drive. (b) Linearized induction motor model.

In order to solve the detuning problem, a plug-in robust compensator, using $\mathcal{H}_\infty$ loop-shaping design technique, was employed to compensate the system degradation due to plant parameter variations and in the presence of external load torque.

III. Controller Design

In a general controller design process, the system plant model is usually not perfectly known. The designer often only knows a nominal model of the plant and a simple controller can be designed to achieve a satisfactory tracking performance for the nominal plant. In this paper, we do not address the issue of how such a controller can be designed. We simply assume that such a controller has already been designed or, in some cases, is even already in operation in the real system. However, it is often the case that this controller may not work well when the plant is perturbed and/or external disturbance presents. In this situation, an additional controller is needed to improve the robustness of the overall system against plant uncertainties and external disturbances. It is desirable that this additional controller can be plugged into the existing control system without dismantling the existing controller and without affecting the already satisfactory nominal tracking performance. This is why we call such an additional controller a plug-in robust compensator. In this section, we propose to design such a plug-in robust compensator using the $\mathcal{H}_\infty$ loop-shaping technique.

A. Controller Structure

Consider the feedback system in Fig. 2(a). Here, P is a single-input–single-output (SISO) strictly proper nominal system and $K = [K_1 - K_2]$ is a 2DOF controller. Assume initially that a

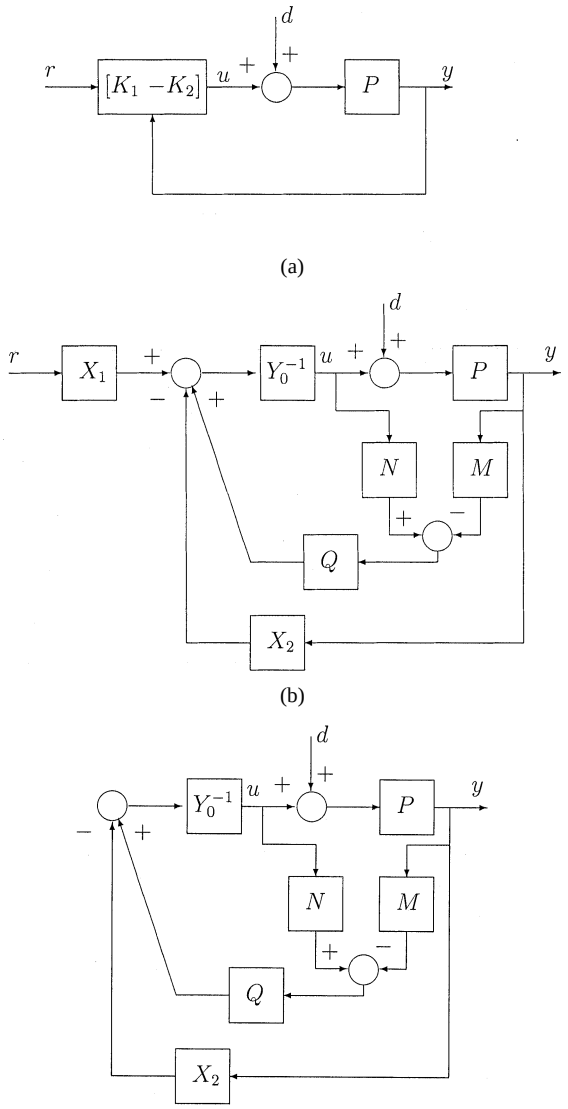

Fig. 2. (a) General 2DOF controller. (b) Proposed plug-in robust compensator. (c) Block digram for the design of the plug-in compensator Q.

controller $K = C = [C_1 - C_2]$ is either already available or in operation with satisfactory nominal tracking performance, i.e., the transfer function from reference r to output y

$$\frac{Y}{R} = \frac{C_1 P}{1 + C_2 P}$$

is satisfactory. How to design C is not the concern of this paper. It can be a simple PI controller tuned in an online fashion or it can be designed by any other methods such as the one given in [8]. Let a coprime factorization of P be given as

$$P = \frac{N}{M}$$

where $M, N \in \mathcal{H}_\infty$. Since C is a stabilizing 2DOF controller for P, for any coprime factorization

$$C = \frac{[X_1 - X_2]}{Y_0}$$

where X_1, X_2 and $Y_0 \in \mathcal{H}_\infty$. It is shown in [15, Sec. 5.6, Th. 15] that all 2DOF stabilizing controllers can be parameterized as

$$[K_1 - K_2] = \frac{[S - (X_2 + QM)]}{(Y_0 - QN)} \tag{9}$$

where $Q \in \mathcal{H}_\infty$ and $S \in \mathcal{H}_\infty$ are arbitrary stable systems. The nominal controller C is obtained when $Q = 0$ and $S = X_1$. The transfer function from r to y, which determines the nominal tracking performance, is

$$\frac{Y}{R} = \frac{NS}{Y_0 M - X_2 N}$$

which is independent of Q. Therefore, the set of all stabilizing 2DOF controllers which gives the same nominal tracking performance is given by

$$[K_1 - K_2] = \frac{[X_1 - (X_2 + QM)]}{(Y_0 - QN)}.$$

The loop property of the feedback system, which depends on K_2 and P only, now depends on Q only. For any stable system Q, which can even be nonlinear and time varying, the nominal tracking performance is unaffected and the closed-loop stability is guaranteed [12], [16]. Suppose that a Q is chosen; theoretically, there are two ways to implement the new controller K. One is to explictly obtain K from (9) and implement as in Fig. 2(a). The other way is to use the structure in Fig. 2(b). Externally, the controllers in Fig. 2(a) and (b) are identical. Internally, they are different. Firstly, if the controller structure shown in Fig. 2(b) is employed, the command tracking performance and the system robustness specification can be designed separately by the blocks X_1, X_2, Y_0 and Q [16]. Hence, this leads to the controller plug-in feature when X_1, X_2, Y_0 form the existing controller while Q is the plug-in robust compensator. Secondly, the output of the block Q can be used as a fault detection signal [7], [17], [18] to estimate and compensate for the system faults and monitor the system deviation from the nominal plant. Finally, the free parameter Q can be changed adaptively using the information provided by the closed-loop system identification to perform the autotuning and further improve the system performance [6].

B. $\mathcal{H}_\infty$ Loop-Shaping Plug-in Compensator Design

Since the purpose of Q is to improve the loop property of the feedback system, the tracking issue is not of concern in its design. The feedback loop part of the whole system is redrawn in Fig. 2(c) with the reference injection part ignored. Fig. 2(c) can be simplified to Fig. 3(a) with $K_2 = (X_2 + QM/Y_0 - QN)$. Our idea in the design of a stable Q is to design a stabilizing K_2 and then back substitute to get Q using

$$Q = \frac{K_2 Y_0 - X_2}{M + K_2 N} \tag{10}$$

which is obtained from (9). Since all stabilizing K_2 are obtained from

$$K_2 = \frac{X_2 + QM}{Y_0 - QN}$$

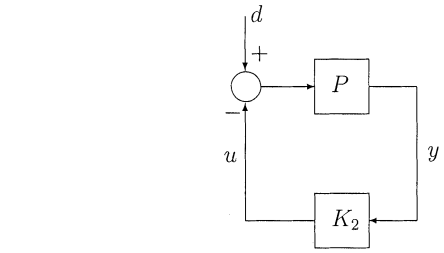

(a)

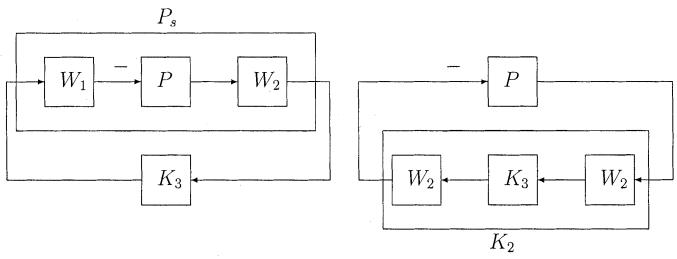

(b)

Fig. 3. (a) Standard feedback configuration. (b) $\mathcal{H}_\infty$ loop-shaping controller design procedure.

over all stable Q, it follows that Q obtained from (10) for a stabilizing K_2 has to be stable.

The design of the controller K_2 is further divided into two steps. The first step is to choose a proper pre-filter W_1 and post-filter W_2 so that the shaped plant, $P_s = W_1 P W_2$, has a desired open-loop frequency response according to some well-defined specifications such as bandwidth or steady state error requirement. Then an $\mathcal{H}_\infty$ optimal robust controller K_3 is found to minimize

$$\left\| \begin{bmatrix} I \\ K_3 \end{bmatrix} (I + P_s K_3)^{-1} [\, I \quad P_s \,] \right\|_\infty . \tag{11}$$

This can be done using the solution in [13] or the command *ncfsyn* of MATLAB μ-Analysis and Synthesis Toolbox [14]. The controller K_2 is obtained by combining the pre-filters W_1, post-filter W_2 and the $\mathcal{H}_\infty$ controller K_3 as $K_2 = W_1 K_3 W_2$. Fig. 3(b) shows the $\mathcal{H}_\infty$ loop-shaping controller design procedure. Finally, the block Q can be found in (10).

The main advantage of the $\mathcal{H}_\infty$ loop-shaping controller over the $\mathcal{H}_\infty$ mixed-sensitivity controller is that the proper selection of the weighting functions, which is difficult in practice, is avoided in the design process. Instead, the pre-filter and post-filter are used to shape the open loop plant to achieve a desired frequency response according to some well defined design specifications such as bandwidth and steady-state error. Furthermore, the time-consuming γ-iteration in computing the optimal robust controller is no longer necessary. Finally, the $\mathcal{H}_\infty$ norm minimization of the four closed-loop transfer functions defined in (11) actually achieves a good balance of the sensitivity and complementary functions so as to improve the overall system robustness against parameter variations such as rotor resistance change in IFOC induction machine drives, motor inertia, and frictional torque change, as well as the disturbance rejection performances against external load torque and sensor noise.

C. Speed Controller Design for the Induction Motor Control System

Following the approach in [8],

$$[C_1(s) - C_2(s)] = \frac{1}{s}[c_{10}s + c_{11} - (c_{20}s + c_{21})]$$

is employed to robustly track a step reference and reject a constant external disturbance. The robustness in tracking a step reference requires $c_{11} = c_{21}$.

For speed control, our plant is a SISO strictly proper stable system. It follows that $M(s) = 1$ and $N(s) = P(s)$ can be assigned and $P(s) = (1/J_m s + B_m)$ is the nominal plant model. Now, the problem is reduced to the choices of proper pre-filter and post-filter. As our plant is a SISO system, we can simply assign $W_2(s) = 1$ and only put emphasis on the choice of $W_1(s)$. As the nominal controller $C_2(s)$ has already had an integrator to reject the constant disturbance, the choice of $W_1(s)$ here is equal to $\alpha C_2(s)$ so that the nominal loop frequency response can be optimized according to the norm in (11), and α is a constant used to adjust the bandwidth of the shaped plant. Since the rotor resistance enters the linear model of the IFOC system in a highly nonlinear way and there are possibly other parameter uncertainties from unknown sources, the selection of the pre-filter does not depend on the structural and magnitude information of the uncertainties. In our design, unstructured uncertainty for IFOC induction drive systems is considered and the pre-filter $W_1(s)$ is chosen to improve the robustness of the overall system that inherently includes that against the rotor resistance change.

In this design example, $Y_0(s) = s/(c_{20}s + c_{21})$, $X_1(s) = (c_{10}s + c_{11}/c_{20}s + c_{21})$, $X_2(s) = 1$, and $P(s) = (1/J_m)/(s + B_m/J_m)$ are first assumed, then the pre-filter is assigned as $W_1(s) = \alpha(c_{20}s + c_{21})/s$. $P_s(s) = \alpha(c_{20} + c_{21})/s(J_m s + B_m)$ is the shaped plant where α is a constant to adjust the bandwidth. Following the solution in [13], the $\mathcal{H}_\infty$ controller, K_3, is a first-order system and the final solution Q can be found from (10).

D. Position Controller Design for the Induction Motor Control System

In a position control system, a desired nominal tracking response can be achieved using a PID controller. The nominal controller C we employ in this section is a 2DOF PID controller

$$[C_1(s) - C_2(s)] = \frac{1}{s}[c_{10}s^2 + c_{11}s + c_{12} - (c_{20}s^2 + c_{21}s + c_{22})].$$

The robustness in tracking a step reference requires $c_{12} = c_{22}$.

The plug-in compensator design is more difficult for position control because the plant is now a SISO strictly proper unstable system. However, our controller design algorithm is still capable of handling such a system. The coprime factorization of the P is first performed and it follows that $N(s) = 1/(\delta_2 s + 1)(J_m s + B_m)$ and $M(s) = s/(\delta_2 s + 1)$ where δ_2 is any positive constant. $P(s) = 1/s(J_m s + B_m)$ is the nominal plant model. Again, the choice of $W_1(s)$ is equal to $\alpha C_2(s)$ so that the controller has an integrator to reject the constant disturbance and α is a constant used to adjust the bandwidth of the shaped plant.

For this position control design example, $Y_0(s) = s/(c_{20}s^2 + c_{21}s + c_{22})$, $X_1(s) = (c_{10}s^2 + c_{11}s + c_{12})/(c_{20}s^2 + c_{21}s + c_{22})$ and $X_2(s) = 1$ can be first assumed, then the pre-filter is assigned as $W_1(s) = \alpha(c_{20}s^2 + c_{21}s + c_{22})/s$. $P_s(s) = \alpha(c_{20}s^2 + c_{21}s + c_{22})/s^2(J_m s + B_m)$ is the shaped plant. Following the solution in [13], the $\mathcal{H}_\infty$ controller, K_3, is a second order stable transfer function and the final solution Q can be found from (10).

TABLE I
MOTOR PARAMETERS

J_m	$0.01111\text{kg}\cdot\text{m}^2$
B_m	$7.355 \times 10^{-4}\text{Nm/rad}\cdot\text{s}^{-1}$
R_r	0.675Ω
R_s	0.76Ω
L_m	$0.2176H$
L_r	$0.2235H$
L_s	$0.2248H$
P	4
Encoder resolution	4096 counts/rev

IV. SIMULATION RESULTS

A 1.5-kW induction motor was used in our simulations and experimental tests. The motor parameters are listed in Table I. To show the effectiveness of the plug-in compensators, the nominal controllers were used for comparison in speed and position control, respectively.

A. Simulation Results for the Speed Controller

In reference to [8], the nominal controller

$$[C_1(s) - C_2(s)] = \frac{1}{s}[0.9028s + 50 - (1.5307s + 50)] \quad (12)$$

was obtained. The corresponding closed-loop poles were located at -84.7262 and -53.1176 respectively while the closed-loop zero was equal to -55.38.

For the design of the block Q defined in Section III, the pre-filter $W_1(s) = \alpha(1.5307s + 50)/s$ was chosen. Fig. 4(a) shows the Bode plot of the pre-filter $W_1(s)$. The constant α was chosen to be 8 so that the crossover frequency of the shaped plant was around 160 Hz as shown in Fig. 4(b), which was adequate for torque rejection loop because the bandwidth of the outer velocity loop was in the order of 10 Hz, generally.

By using the command *ncfsyn* of MATLAB μ-Analysis and Synthesis Toolbox, $K_3(s) = (1.02s + 31.75/s + 32.65)$ was found and then from (10), the optimal plug-in compensator

$$Q(s) = \frac{7.2267s(s + 30.63)(s + 0.0662)}{(s + 1102)(s + 32.68)(s + 31.75)} \quad (13)$$

was obtained.

In the following simulation experiments, the nominal controller defined in (12) without the plug-in compensator was used for comparison. In the first simulation, a constant reference speed $r = 1000$ r/min was applied at 2 s, so that the constant rotor flux condition can be assumed. Fig. 5(a) shows the simulation results and we found that the transient tracking

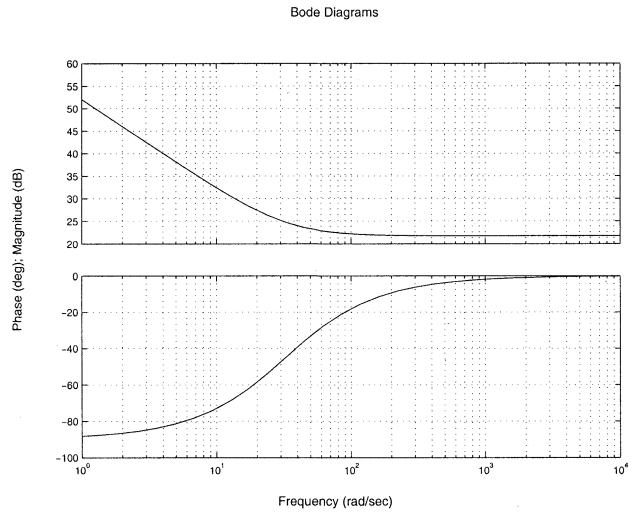

(a)

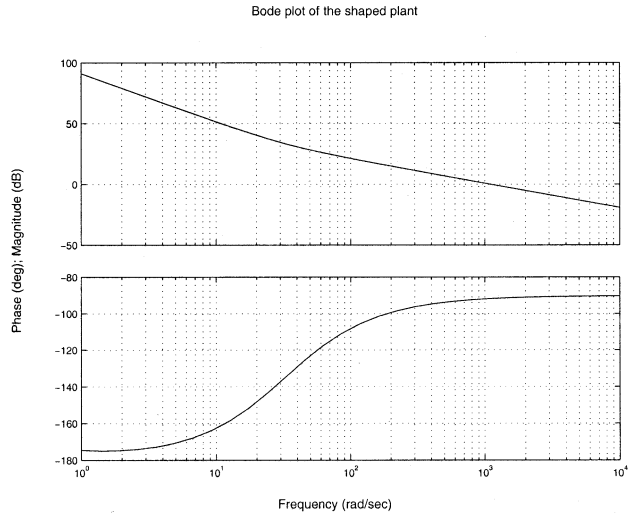

(b)

Fig. 4. (a) Bode plot of the prefilter W_1. (b) Bode plot of the shaped plant $P_s = W_1 P$.

performance was not affected by the addition of the plug-in compensator.

Then, a 2-N·m load torque was applied at 2.5 s. The upper section of Fig. 5(b) shows the speed responses of the nominal controller and the one with the plug-in robust compensator. It is clear that the external torque can be rejected faster with the addition of the proposed plug-in robust compensator. The lower section of Fig. 5(b) shows the speed response when the rotor resistance R_r was doubled suddenly at three seconds while the load torque was still being applied. Without the help of the plug-in robust compensator, the output speed oscillates with amplitude approximately equals ± 20 r/min; however, the output speed only shakes slightly and settles down quickly when the proposed plug-in robust compensator was used. Fig. 5(c) shows the phase—A current and the command current i_{qs}^{e} for the proposed plug-in compensator. Both of them are within the current limit of the motor driver and the motor winding and this validates that the proposed controller can be implemented practically.

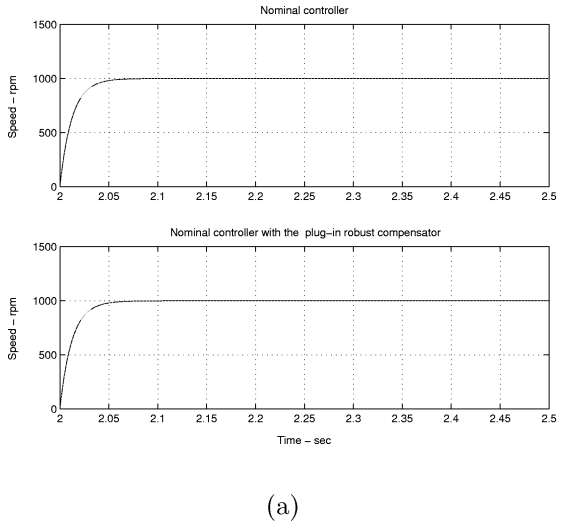

(a)

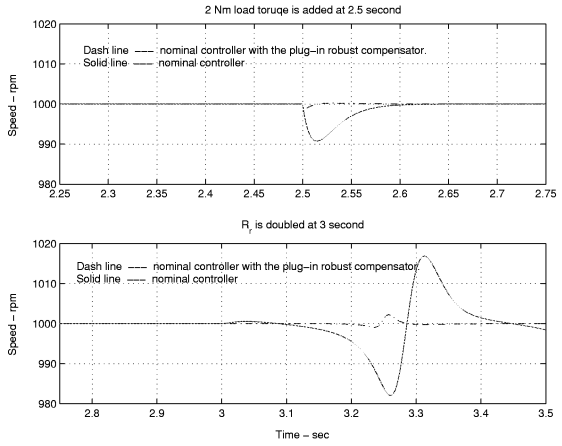

(b)

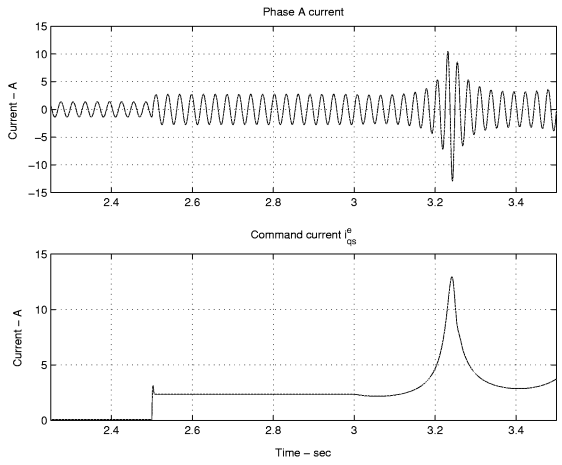

(c)

Fig. 5. Speed control. (a) Transient tracking response comparison. (b) System robustness test. (c) Phase-A current and command current i_{qs}^{e*}.

From the simulation results, there is no doubt that the disturbance rejection performance and robustness against plant pa-

rameter variations have both been improved by using the plug-in robust compensator. The only extra cost is the implementation of the extra linear blocks Q and P_0.

B. Simulation Results for the Position Controller

The nominal controller for position loop control

$$[C_1(s) - C_2(s)] = \frac{1}{s}[0.58s^2 + 103s + 4600 - (2.55s^2 + 190s + 4600)] \quad (14)$$

was obtained to robustly track a step reference and reject a constant external disturbance. The corresponding closed-loop poles were approximately located at $-88.56 \pm j7.63$ and -52.4, respectively, while the closed-loop zeros were approximately equal to $-88.56 \pm j8.23$.

For the design of the block Q defined in Section III, the pre-filter $W_1(s) = 4(2.55s^2 + 190s + 4600)/s$ was chosen. As described in Section IV-A, the constant α was chosen to be 4 so that the cross-over frequency of the shaped plant was around 160 Hz, which was adequate for torque rejection loop because the bandwidth of the outer position loop was in the order of 10 Hz, generally.

By using the command *ncfsyn* of MATLAB μ-Analysis and Synthesis Toolbox again, the $\mathcal{H}_\infty$ controller

$$K_3(s) = \frac{1.0761(s^2 + 67.55s + 1556)}{(s^2 + 74.48s + 1802)}$$

was found and then from (10), the optimal plug-in robust compensator

$$Q(s) = \frac{33 \times 10^{-4} s(s + 1000)(s^2 + 65.34s + 1482)(s + 0.0662)}{(s + 917)(s^2 + 74.86s + 1804)(s^2 + 70.91s + 1675)}$$

was obtained. Using the Hankel norm model reduction with dc gain matching [10], we obtain a third-order approximation of the optimal plug-in robust compensator

$$Q(s) \approx \frac{33 \times 10^{-4} s(s + 978.1)(s + 0.1092)}{(s + 896.5)(s^2 + 80.59s + 2054)}. \quad (15)$$

In the following simulation experiments, the nominal controller without the plug-in compensator in (14) was used for comparison. A constant reference position $r = 2\pi$ rad was applied at 2 s, so that the constant rotor flux condition can be assumed. Fig. 6(a) shows the simulation results. We found that the transient tracking response was not affected by the addition of the plug-in robust compensator.

Next, a 2-N·m load torque was applied at 2.5 s. The upper section of Fig. 6(b) shows the position responses of the nominal controller alone and the one with the plug-in robust compensator. It is clear that disturbance rejection performance is much better with the help of the plug-in robust compensator. In addition, the output performance of the approximation of the optimal plug-in compensator is almost the same as that of the optimal plug-in compensator.

The lower section of Fig. 6(b) shows the position response when the rotor resistance R_r was doubled suddenly at 3 s while the load torque was still being applied. Without the help of the plug-in robust compensator, the output position oscillates significantly; however, the output position is almost not affected when

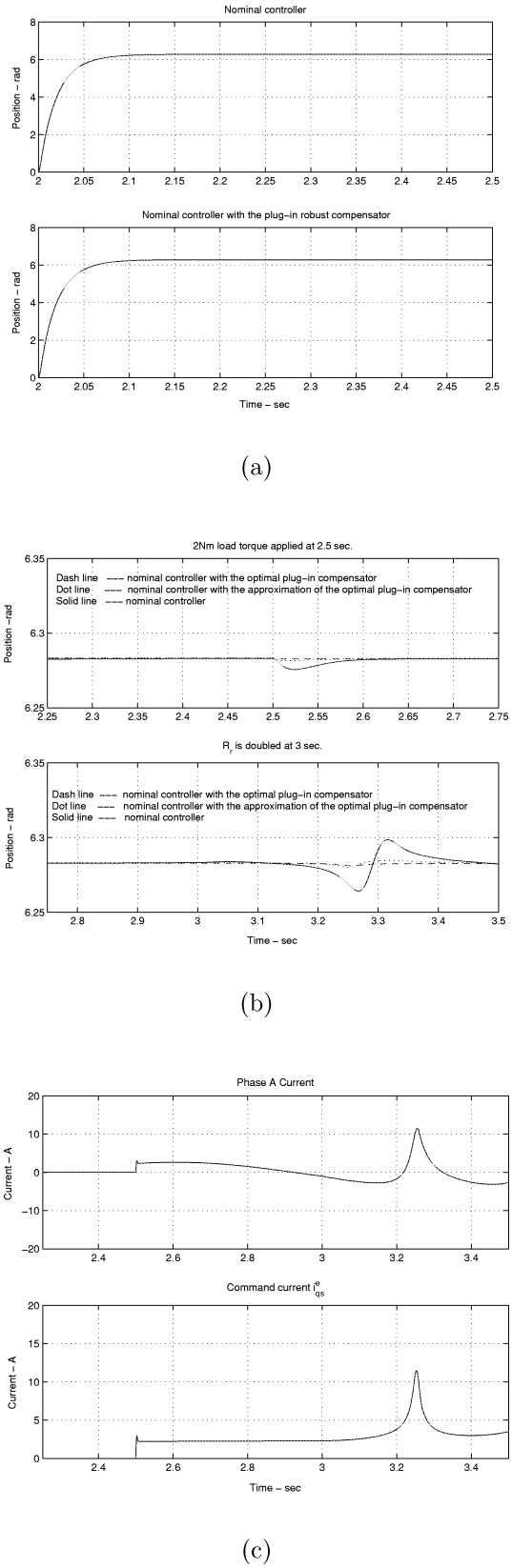

Fig. 6. Position control. (a) Transient tracking response comparison. (b) System robustness test. (c) Phase-A current and command current i_{qs}^{e*}.

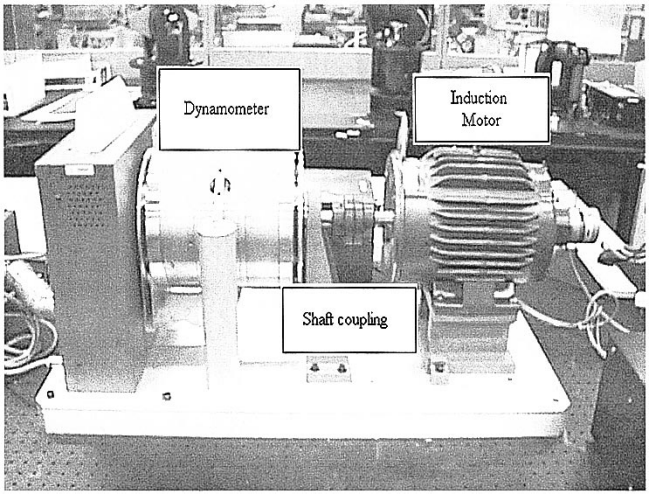

Fig. 7. Motor test platform at HKUST.

the proposed plug-in robust compensator was used. Fig. 6(c) shows the phase A current and the command current i_{qs}^{e} for the approximation of the optimal plug-in compensator. Both of them are within the current limit of the motor driver and the motor winding.

The simulation results in this section show the effectiveness of the proposed plug-in compensator. It is clear that the proposed compensator can greatly enhance the system robustness for an IFOC induction motor drive system. The mechanical outputs (speed and position) are recorded to illustrate the desirable system response while the internal electrical variables such as i_{qs}^{e} and i_{as} are also captured for inspection to ensure that the internal stability remains.

V. Experimental Results

Experiments are performed to verify the effectiveness of our proposed controllers. Basically, the hardware setup is constructed as in Fig. 1(a). A dSPACE DS1102 DSP controller board was used as our motion controller to implement the velocity/position controller and the IFOC algorithm. In connection with MATLAB real-time workshop and SIMULINK, a fast prototyping working environment was achieved and hence the code development time can be saved. The DSP controller implements all control algorithms with a sampling frequency 2 kHz. In every control cycle, the controller reads the motor encoder, performs the control algorithm calculation and then outputs two phase current reference commands to the current tracking amplifier. An Advanced Motion Controls Inc. S30A40B current-tracking driver was used and the 1.5-kW three-phase induction motor was from Baldor Inc. with the parameters listed in Table I. A Magtrol Inc. dynamometer was used to generate the load torque in this experiment. Fig. 7 shows the induction motor under a load torque test at the motor control laboratory in the Hong Kong University of Science and Technology (HKUST).

The proposed plug-in robust compensators, (13) and (15), and the nominal controllers of speed and position control, (12) and (14), stated in Section IV were used in the actual experiment. In total, there were six experiments conducted to verify the effectiveness of the proposed compensator.

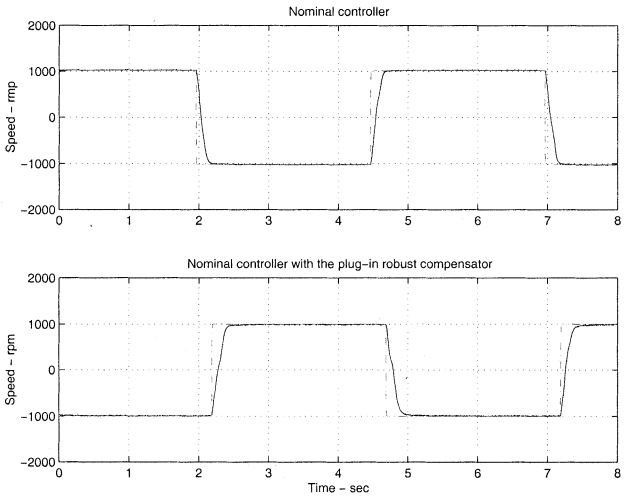

(a)

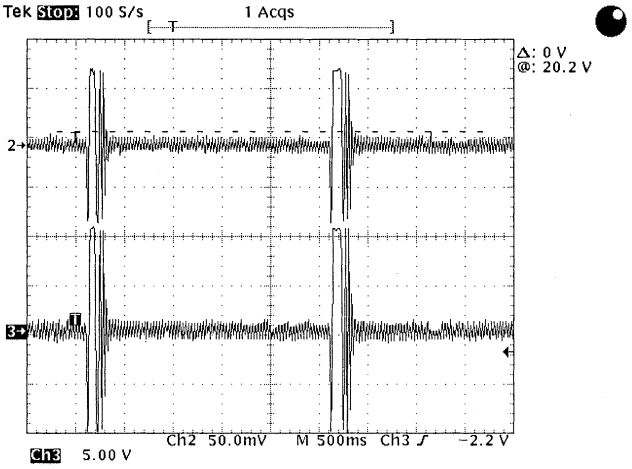

(b)

Fig. 8. Speed control. (a) Transient tracking response comparison. (b) Channel 2: actual phase-A current (10 A/div); channel 3: phase–A current command.

A. Experimental Results for the Speed Controller

Fig. 8(a) shows the speed-tracking performance without any load disturbances and plant parameter variations. As mentioned in Section III, the plug-in compensator does not affect the transient tracking response. The current tracking response is shown in Fig. 8(b) for one reference cycle when the plug-in compensator was turned on. The actual current tracks closely with the command value. This proves the current loop bandwidth is adequate for our application and the internal electrical current behaves satisfactorily with the plug-in compensator.

With a fully computer-controlled dynamometer, a step load can be easily applied to the motor system in order to verify the disturbance rejection performance. Fig. 9(a) shows the experimental results, it is clear that the system controlled using the plug-in compensator did not have any significant speed drop under a 2-N·m load torque; however, a 30-r/min speed drop and a 0.3-s recovery time resulted if the nominal controller was used alone. The current commands i_{qs}^{e} of the nominal controller and

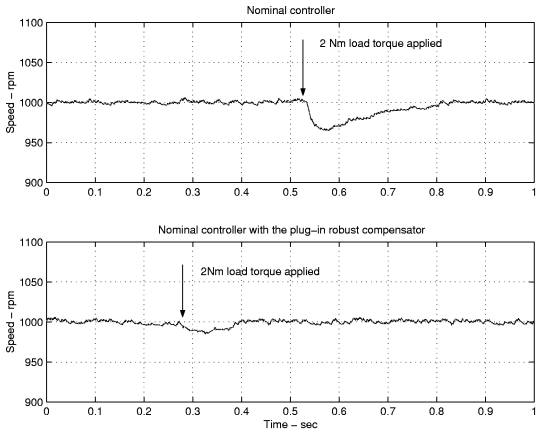

(a)

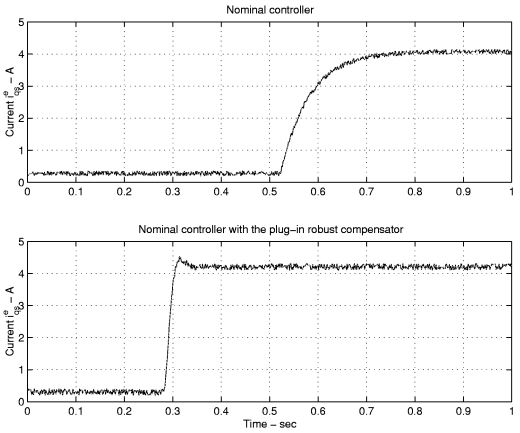

(b)

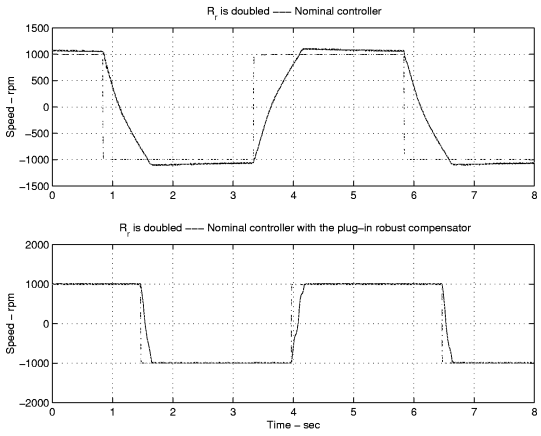

(c)

Fig. 9. Speed control. (a) Disturbance rejection comparison. (b) Current command i^e_{qs} comparison. (c) Speed tracking response comparison under plant parameter variation.

the one with the plug-in compensator are shown in Fig. 9(b), it can be observed that the torque compensation using the plug-in

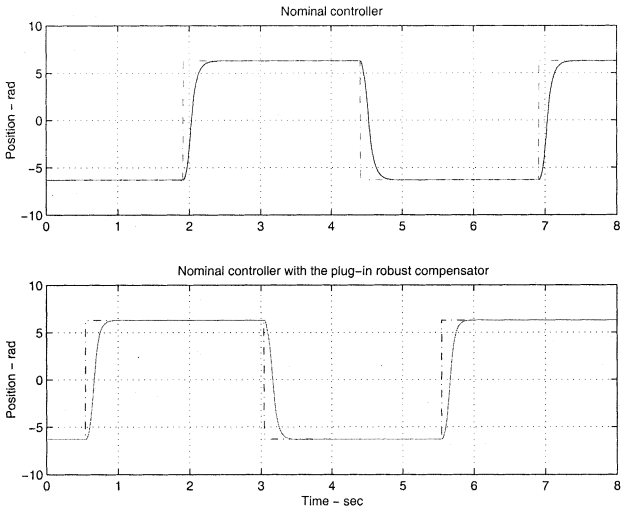

(a)

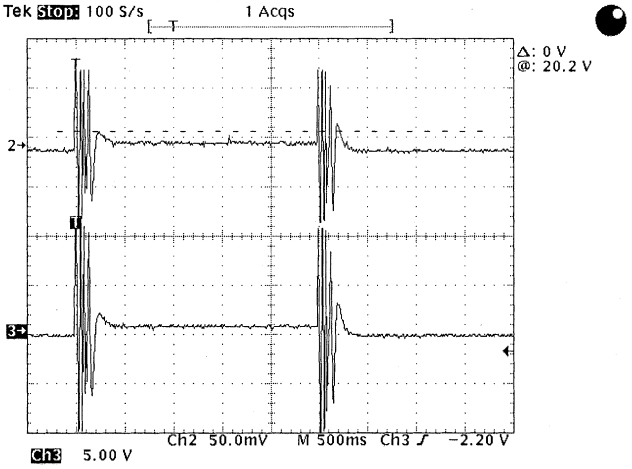

(b)

Fig. 10. Position control. (a) Transient tracking response comparison. (b) Channel 2: actual phase-A current (10 A/div); channel 3: phase-A current command.

compensator is much faster than that of the nominal controller and hence the speed regulation can still be maintained.

The third experiment is to verify how the plug-in robust compensator can improve the system performance under plant parameter variations. In this experiment, the value R_r in the controller was artificially doubled and then the output speed response was recorded. Fig. 9(c) shows the experimental results. From the upper section of Fig. 9(c), the nominal controller cannot compensate the plant parameter variation and hence the rise time is prolonged. In addition, the overshoot and steady-state error are present. If the plug-in robust compensator was used, the output speed response did not show any significant degradation under the plant parameter variations.

B. Experimental Results for the Position Controller

Fig. 10(a) shows the position-tracking performance without any load disturbance and plant parameter variations. The addition of the plug-in compensator does not affect the transient tracking response. The current tracking response for phase

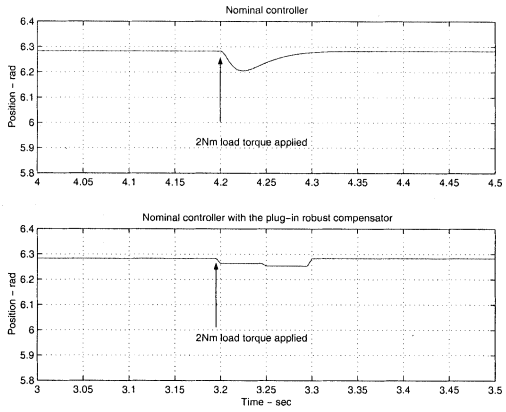

(a)

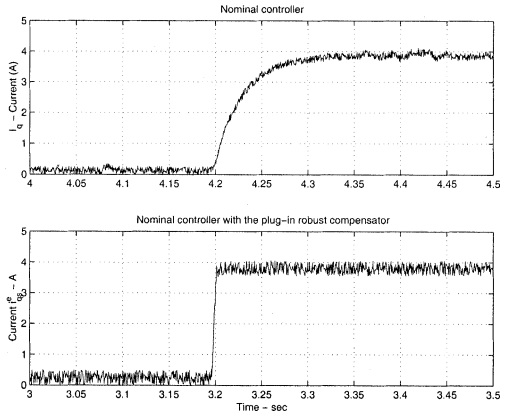

(b)

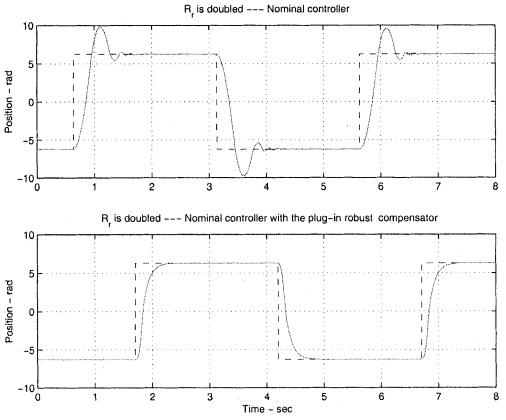

(c)

Fig. 11. Position control. (a) Disturbance rejection comparison. (b) Current command i_{qs}^{e} comparison. (c) Position tracking response comparison under plant parameter variation.

winding A is shown in Fig. 10(b) for one reference cycle when the plug-in compensator was turned on. The actual current tracks closely with the command value and falls within the driver and motor limit. This proves the internal electrical current is still stable when the plug-in compensator was on.

As in the speed-loop load-torque test, a step load torque was applied using a dynamometer. Fig. 11(a) shows the experimental results; it is clear that the system controlled with the plug-in compensator did not have any significant position variation under a 2-N·m load torque; however, a 0.1-rad position variation was recorded if the nominal controller was used alone. The current commands i_{qs}^{e} of the nominal controller and the one with the plug-in compensator are shown in Fig. 11(b). It can be observed that the torque compensation using the plug-in compensator is much faster than that using the nominal controller alone and, hence, the position regulation can still be maintained.

The final experiment in this section is to verify the robustness enhancement of the proposed plug-in compensator. In this experiment, the value R_r in the controller was artificially doubled and then the output position response was measured. Fig. 11(c) shows the experimental results. There are overshoots and oscillations in the transient tracking response if the nominal controller was used alone. However, a good tracking response with no overshoot was achieved by turning on the plug-in compensator although the rise time is prolonged slightly.

From the above experimental results, we found that the results match well with the simulation results in Section IV. This validates the effectiveness of the proposed plug-in robust compensator.

VI. Conclusions

In this paper, a simple and effective method is proposed for the design of a plug-in robust compensator for IFOC induction machine drives. With this plug-in robust compensator, the IFOC induction machine drivers achieve good system output responses even under plant parameter variations such as rotor resistance change and in the presence of the external disturbances.

The nominal command tracking response and the system robustness performance of the proposed controller can be designed separately [16]. The nominal command tracking response can be taken care using simple nominal or existing controllers such as PID and lead–lag compensators while the system robustness and the disturbance rejection response can be improved using the proposed plug-in robust compensator. In the design of the plug-in compensator, the $\mathcal{H}_\infty$ loop-shaping technique is employed to compensate for the unstructured model uncertainties such as the rotor resistance change in IFOC machine drives that is difficult to model. In comparison to other robust controller design, the selection of the weighting functions in $\mathcal{H}_\infty$ loop-shaping controller design is sample as the weighting functions are chosen according to some well-defined system specifications such as bandwidth and steady-state error requirement. In addition, the $\mathcal{H}_\infty$ loop-shaping controller can be found without any iterative computation.

The proposed plug-in robust compensator is not only applicable for IFOC induction motor drive systems, but is also capable of handling more general systems subject to disturbance and modeled/un-modeled uncertainties. The proposed plug-in compensator had been successfully applied to an accurate position control of a linear switched reluctance motor [19]. In addition, the input and output signals of the block Q can be used for fault tolerant control [7], [17], [18] and, hence, a more reliable system can be achieved.

REFERENCES

[1] D. W. Novotny and T. A. Lipo, *Vector Control and Dynamics of AC Drives*. Oxford, U.K.: Clarendon, 1998.

[2] K. B. Nordin, D. W. Novotny, and D. S. Zinger, "The influence of motor parameter deviations in feedforward field orientation drive systems," *IEEE Trans. Ind. Applicat.*, vol. IA-21, pp. 1009–1015, July/Aug. 1985.

[3] Y. T. Kao and C. H. Liu, "Analysis and design of microprocessor-based vector-controlled induction motor drives," *IEEE Trans. Ind. Electron.*, vol. 39, pp. 46–54, Feb. 1992.

[4] B. Heber, L. Xu, and Y. Tang, "Fuzzy logic enhanced speed control of an indirect field-oriented induction machine drive," *IEEE Trans. Power Electron.*, vol. 12, pp. 772–778, Sept. 1997.

[5] T. Ahmed-Ali, F. Lamnabhi-Lagarrigue, and R. Ortega, "A globally-stable adaptive field-oriented controller for current-fed induction motors," in *Proc. American Control Conf.*, vol. 3, 1998, pp. 1498–1502.

[6] T. Ogawa, T. Suzuki, K. Matsumoto, S. Okuma, K. Kamiyama, and K. Ohno, "Internal structure of two-degree-of-freedom controller and its application to vibration suppression control," in *Proc. IEEE IECON'93*, vol. 3, 1993, pp. 2138–2143.

[7] T. Suzuki and M. Tomizuka, "Joint synthesis of fault detector and controller based on structure of two-degree-of-freedom control system," in *Proc. 39th IEEE Conf. Decision and Control*, vol. 4, 1999, pp. 3599–3604.

[8] W. C. Gan and L. Qiu, "Robust two degree of freedom regulators for velocity ripple elimination of AC permanent magnet motors," in *Proc. Ninth IEEE Int. Conf. Control Applications*, vol. 1, Sept. 2000, pp. 156–161.

[9] T. Umeno and Y. Hori, "Robust speed control of DC servomotors using modern two degree-of-freedom controller design," *IEEE Trans. Ind. Electron.*, vol. 38, pp. 363–368, Oct. 1991.

[10] K. Zhou and J. C. Doyle, *Essentials of Robust Control*. Upper Saddle River, NJ: Prentice-Hall, 1998.

[11] G. Vinnicombe, *Uncertainty and Feedback $\mathcal{H}_\infty$ Loop-Shaping and the ν-Gap Metric*. London, U.K.: Imperial College Press, 2001.

[12] P. P. Khargonekar and K. R. Poolla, "Uniformally optimal control of linear time-invariant plants: Nonlinear time-varying controllers," *Syst. Control Lett.*, vol. 6, no. 5, pp. 303–308, 1986.

[13] D. C. McFarlane and K. Glover, *Robust Controller Design Using Normalized Coprime Factor Plant Descriptions*. Berlin, Germany: Springer-Verlag, 1990.

[14] G. J. Balas, J. C. Doyle, K. Glover, A. Packard, and R. Smith, *μ-Analysis and Synthesis Toolbox*. Natick, MA: The MathWorks, Inc, 1994.

[15] M. Vidyasagar, *Control System Synthesis*. Cambridge, MA: MIT Press, 1985.

[16] K. Zhou and Z. Ren, "A new controller architecture for high performance, robust, adaptive, and fault tolerant control," *IEEE Trans. Automat. Contr.*, vol. 46, pp. 1613–1618, Oct. 2000.

[17] D. U. Campos-Delgado and K. Zhou, "Fault tolerant control of a gyroscope system," in *Proc. American Control Conf.*, vol. 4, 2001, pp. 2688–2693.

[18] X. Ding and P. M. Frank, "Fault detection via factorization approach," *Syst. Control Lett.*, vol. 14, no. 5, pp. 431–436, 1990.

[19] W. C. Gan, N. C. Cheung, and L. Qiu, "Short distance position control for linear switched reluctance motors: A plug-in robust compensator approach," in *Conf. Rec. IEEE-IAS Annu. Meeting*, vol. 4, Oct. 2001, pp. 2329–2336.

Wai-Chuen Gan (S'94–M'02) received the B.Eng. degree, with first class honors and academic achievement award, in electronic engineering and the M.Phil. and Ph.D. degrees in electrical and electronic engineering from The Hong Kong University of Science and Technology, Hong Kong, in 1995, 1997, and 2001, respectively.

From 1997 to 1999, he was with ASM Assembly Automation Ltd., Hong Kong, as a Motion Control Application Engineer. He rejoined the company in 2002 and is currently responsible for the development of the digital motor drivers. His current research interests include robust control of ac machines, power electronics, design and control of linear switched reluctance motors, and control of stepping motors via interconnection and damping assignment.

Li Qiu (S'85–M'90–SM–'98) received the B.Eng. degree in electrical engineering from Hunan University, Changsha, China, in 1981, and the M.A.Sc. and Ph.D. degrees in electrical engineering from the University of Toronto, Toronto, ON, Canada, in 1987 and 1990, respectively.

Since 1993, he has been an Assistant Professor and then an Associate Professor in the Department of Electrical and Electronic Engineering, The Hong Kong University of Science and Technology, Hong Kong. He has also held research and teaching positions with the University of Toronto, Canadian Space Agency, University of Waterloo, University of Minnesota, Zhejiang University, and Australia Defence Force Academy. His current research interests include systems control theory, signal processing, and motor control.

Dr. Qiu served as an Associate Editor of the IEEE TRANSACTIONS ON AUTOMATIC CONTROL and of *Automatica*.